Supplementary information

Inactivating *CUX1* mutations promote tumorigenesis

Chi C. Wong[1, 2], Inigo Martincorena[3], Alistair G. Rust[1], Mamunur Rashid[1], Constantine Alifrangis[4], Ludmil B. Alexandrov[3], Jessamy C. Tiffen[1], Christina Kober[1], Chronic Myeloid Disorders Working Group of the International Cancer Genome Consortium[5], Anthony R. Green[2, 6, 7], Charles E. Massie[2, 6, 7], Jyoti Nangalia[2, 6, 7], Stella Lempidaki[8], Hartmut Döhner[9], Konstanze Döhner[9], Sarah J. Bray[8], Ultan McDermott[4], Elli Papaemmanuil[3], Peter J. Campbell[2, 3] & David J. Adams[1*]

[1]Experimental Cancer Genetics, Wellcome Trust Sanger Institute, Hinxton, Cambridge, CB10 1SA, UK. [2]Department of Haematology, University of Cambridge, Hills Road, Cambridge, CB2 0SP, UK. [3]The Cancer Genome Project, Wellcome Trust Sanger Institute, Hinxton, Cambridge, CB10 1SA, UK. [4]The Cancer Translation Project, Wellcome Trust Sanger Institute, Hinxton, Cambridge, CB10 1SA, UK. [5]See Supplementary Note for members and affiliations, [6]Cambridge Institute for Medical Research, University of Cambridge, Hills Road, Cambridge, CB2 0SP, UK. [7]Wellcome Trust/MRC Stem Cell Institute, University of Cambridge, Cambridge, UK. [8]Department of Physiology, Development and Neuroscience, University of Cambridge, CB2 3DY, UK. [9]Department of Internal Medicine III, University of Ulm, Albert-Einstein-Allee 23 89081, Ulm, Germany.

SUPPLEMENTARY NOTE

Members of Chronic Myeloid Disorders Working Group of the International Cancer Genome Consortium

Luca Malcovati & Mario Cazzola, Fondazione IRCCS Policlinico San Matteo, University of Pavia, Pavia, Italy; Eva Hellstrom-Lindberg, Department of Haematology, Karolinska Institute, Stockholm, Sweden; David Bowen, St. James Institute of Oncology, St. James Hospital, Leeds, UK; Paresh Vyas, Weatherall Institute of Molecular Medicine, University of Oxford, UK; Carlo Gambacorti-Passerini, Department of Haematology, University of Milan Bicocca, Milan, Italy; Nicholas C. P. Cross, Faculty of Medicine, University of Southampton, Southampton, UK; Anthony R. Green, Department of Haematology, University of Cambridge, UK & Department of Haematology, Addenbrooke's Hospital, Cambridge, UK; Jacqueline Boultwood, Nuffield Department of Clinical Laboratory Sciences, University of Oxford, UK.

Role of *CUX1* in cancer

Higher levels of *CUX1* expression have been detected in breast[1], pancreatic[2] and colon[3] cancer tissues and are associated with advanced tumor grade and aggressiveness, supporting an oncogenic role for *CUX1*. Additionally, transgenic mouse lines overexpressing $Cux1^{p75}$ or $Cux1^{p110}$ isoforms manifest an array of phenotypes including multi-organ organomegaly, kidney abnormalities, cancerous liver lesions, myeloproliferation and mammary tumors after long latency[4-10]. In contrast, mutations predicted to generate truncated $CUX1^{p200}$ and derivative $CUX1^{p110}$ proteins are expected to be transcriptionally inactive due to the absence of nuclear localization sequences near the C-terminal homeodomain[11,12]. In addition, knockdown of CUX1 expression in human hematopoietic cells increased their engraftment capability in immunodeficient mice[13], consistent with a tumor suppressive role for *CUX1*.

Role of *CUX1* in T-ALL

Although our results were consistent with *CUX1* being a tumor suppressor, it was curious that transposon tumors with *Cux1* insertions had a T-ALL phenotype, yet *CUX1* mutations appear to be associated with myeloid malignancy in humans. Perhaps this may be ascribed to species differences, but notably 17/20 tumors with *Cux1* insertions also had prototypical insertions in potent T-ALL cancer genes such as *Notch1*, *Ikzf1* or *Pten* (see **Supplementary Fig. 3**), which can drive T-ALL development as independent lesions[14-16]. Interestingly however, *CUX1* truncation as a result of chromosomal translocation has been described in human T-ALL[17] and we detected two *CUX1* mutations by Sanger sequencing of *CUX1* coding exons in eight human T-ALL cell lines, including one heterozygous truncating variant (see **Supplementary Fig. 10**), suggesting a tumor suppressive role for *CUX1* in human T-ALL. In support, adoptive transfer experiments using CUX1-knockdown human hematopoietic cells revealed a role for *CUX1* in T-cell and myeloid lineages[13].

Supplementary Discussion

Other candidate tumor suppressor genes identified in our approach included *ARHGAP35*, *AMOT*, *MGA* and *LARP4B*. In the cases of *ARHGAP35* and *AMOT*, functional data consistent with these genes being tumor suppressors has been reported[18,19], but until now they have not been shown to be recurrently mutated. *MGA*, encoding a Myc repressor[20], has been found to be mutated in a small cohort of chronic lymphocytic leukemias[21,22], but our study suggests a broader role for *MGA* in multiple cancer types (**Supplementary Table 8**). For *LARP4B*, which appears to be involved in protein translation[23], no link with cancer has been postulated.

Remarkably, the majority of *CUX1* mutations in myeloid disorders were heterozygous. Although, we were unable to exclude silencing of the remaining *CUX1* allele by epigenetic mechanisms, residual *CUX1* expression is retained in -7/del(7q) AML cases[13], concordant with our mouse tumor and cell line analysis. Whether *CUX1* operates predominantly as a haploinsufficient tumor suppressor in other tumor types requires further study. Interestingly, inactivating mutations in the histone methyltransferase *EZH2*, which resides distal to *CUX1* on chromosome 7 at 7q36, have also been identified in myeloid disorders[24,25]. Thus chromosome 7q harbors at least two myeloid tumor suppressor genes consistent with the presence of heterogeneous commonly deleted regions between del(7q) AML samples. *EZH2* mutations also confer poor prognosis in MDS, but in contrast to *CUX1*, homozygous *EZH2* mutations are prevalent[24,26]. Like *EZH2,* which has also been reported to be an oncogene[27], our data reveal that *CUX1* is a member of a growing list of genes, that also includes *USP9X* (refs. 28, 29), *NKX2-1* (refs. 30, 31) and *ZBTB7A* (refs. 32, 33), that may function as both tumor suppressors and oncogenes. The effect of specific *CUX1* mutations is likely to depend on factors such as the expression pattern of CUX1 isoforms and co-operating genetic aberrations in the target cell.

Supplementary References

1. Michl, P. *et al.* CUTL1 is a target of TGF(beta) signaling that enhances cancer cell motility and invasiveness. *Cancer Cell* **7,** 521–532 (2005).
2. Ripka, S. *et al.* CUX1: target of Akt signalling and mediator of resistance to apoptosis in pancreatic cancer. *gut.bmj.com*
3. Muzny, D. M. *et al.* Comprehensive molecular characterization of human colon and rectal cancer. *Nature* **487,** 330–337 (2012).
4. Ledford, A. W. *et al.* Deregulated expression of the homeobox gene Cux-1 in transgenic mice results in downregulation of p27(kip1) expression during nephrogenesis, glomerular abnormalities, and multiorgan hyperplasia. *Dev. Biol.* **245,** 157–171 (2002).
5. Brantley, J. G., Sharma, M., Alcalay, N. I. & Heuvel, G. B. V. Cux-1 transgenic mice develop glomerulosclerosis and interstitial fibrosis. *Kidney Int.* **63,** 1240–1248 (2003).
6. Cadieux, C. *et al.* Transgenic mice expressing the p75 CCAAT-displacement protein/Cut homeobox isoform develop a myeloproliferative disease-like myeloid leukemia. *Cancer Res.* **66,** 9492–9501 (2006).
7. Cadieux, C. *et al.* Polycystic kidneys caused by sustained expression of Cux1 isoform p75. *J. Biol. Chem.* **283,** 13817–13824 (2008).
8. Cadieux, C. *et al.* Mouse mammary tumor virus p75 and p110 CUX1 transgenic mice develop mammary tumors of various histologic types. *Cancer Res.* **69,** 7188–7197 (2009).
9. Siam, R. *et al.* Transcriptional activation of the Lats1 tumor suppressor gene in tumors of CUX1 transgenic mice. *Mol. Cancer* **8,** 60 (2009).
10. Vanden Heuvel, G. B. *et al.* Hepatomegaly in transgenic mice expressing the homeobox gene Cux-1. *Mol. Carcinog.* **43,** 18–30 (2005).
11. Ellis, T. The transcriptional repressor CDP (Cutl1) is essential for epithelial cell differentiation of the lung and the hair follicle. *Genes Dev.* **15,** 2307–2319 (2001).
12. Luong, M. X. *et al.* Genetic Ablation of the CDP/Cux Protein C Terminus Results in Hair Cycle Defects and Reduced Male Fertility. *Mol. Cell. Biol.* **22,** 1424–1437 (2002).
13. McNerney, M. E. *et al.* CUX1 is a haploinsufficient tumor suppressor gene on chromosome 7 frequently inactivated in acute myeloid leukemia. *Blood* **121,** 975–983 (2013).
14. Pear, W. S. *et al.* Exclusive development of T cell neoplasms in mice transplanted with bone marrow expressing activated Notch alleles. *J. Exp. Med.* **183,** 2283–2291 (1996).
15. Winandy, S., Wu, P. & Georgopoulos, K. A dominant mutation in the Ikaros gene leads to rapid development of leukemia and lymphoma. *Cell* **83,** 289–299 (1995).

16. Suzuki, A. *et al.* T Cell-Specific Loss of Pten Leads to Defects in Central and Peripheral Tolerance. *Immunity* **14,** 523–534 (2001).
17. Wasag, B., Lierman, E., Meeus, P., Cools, J. & Vandenberghe, P. The kinase inhibitor TKI258 is active against the novel CUX1-FGFR1 fusion detected in a patient with T-lymphoblastic leukemia/lymphoma and t(7;8)(q22;p11). *Haematologica* **96,** 922–926 (2011).
18. Ludwig, K. & Parsons, S. J. The Tumor Suppressor, p190RhoGAP, Differentially Initiates Apoptosis and Confers Docetaxel Sensitivity to Breast Cancer Cells. *Genes & Cancer* **2,** 20–30 (2011).
19. Zhao, B. *et al.* Angiomotin is a novel Hippo pathway component that inhibits YAP oncoprotein. *Genes Dev.* **25,** 51–63 (2011).
20. Hurlin, P. J. Mga, a dual-specificity transcription factor that interacts with Max and contains a T-domain DNA-binding motif. *EMBO J.* **18,** 7019–7028 (1999).
21. Edelmann, J. *et al.* High-resolution genomic profiling of chronic lymphocytic leukemia reveals new recurrent genomic alterations. *Blood* **120,** 4783–4794 (2012).
22. De Paoli, L. *et al.* MGA, a suppressor of MYC, is recurrently inactivated in high risk chronic lymphocytic leukemia. *Leuk. Lymphoma* **54,** 1087–1090 (2013).
23. Schäffler, K. *et al.* A stimulatory role for the La-related protein 4B in translation. *RNA* **16,** 1488–1499 (2010).
24. Ernst, T. *et al.* Inactivating mutations of the histone methyltransferase gene EZH2 in myeloid disorders. *Nat. Genet.* **42,** 722–726 (2010).
25. Nikoloski, G. *et al.* Somatic mutations of the histone methyltransferase gene EZH2 in myelodysplastic syndromes. *Nat. Genet.* **42,** 665–667 (2010).
26. Bejar, R. *et al.* Clinical effect of point mutations in myelodysplastic syndromes. *N Engl J Med* **364,** 2496–2506 (2011).
27. Xu, K. *et al.* EZH2 Oncogenic Activity in Castration-Resistant Prostate Cancer Cells Is Polycomb-Independent. *Science* **338,** 1465–1469 (2012).
28. Pérez-Mancera, P. A. *et al.* The deubiquitinase USP9X suppresses pancreatic ductal adenocarcinoma. *Nature* **486,** 266–270 (2012).
29. Schwickart, M. *et al.* Deubiquitinase USP9X stabilizes MCL1 and promotes tumour cell survival. *Nature* **463,** 103–107 (2009).
30. Winslow, M. M. *et al.* Suppression of lung adenocarcinoma progression by Nkx2-1. *Nature* **473,** 101–104 (2011).
31. Weir, B. A. *et al.* Characterizing the cancer genome in lung adenocarcinoma. *Nature* **450,** 893–898 (2007).
32. Wang, G. *et al.* Zbtb7a suppresses prostate cancer through repression of a Sox9-dependent pathway for cellular senescence bypass and tumor invasion. *Nat. Genet.* **45,** 739–746 (2013).
33. Maeda, T. *et al.* Role of the proto-oncogene Pokemon in cellular transformation and ARF repression. *Nature* **433,** 278–285 (2005).

a

Diagnoses of MPN cases (n = 151)

48 polycythemia vera; 62 essential thrombocythemia; 39 myelofibrosis; 2 MPN unclassified

Characteristics of AML cohort (n = 1630)

Average age = 48.2 years
Trial distribution: AMLSG 07-04 = 49%; AMLSG 98A = 41%; AMLSG 98B = 10%
Sex = 53% male
AML karyotype: t(15;17) = 4%; t(8;21) = 4%; inv(16)/t(16;16) = 5%; unsuccessful = 9%
-7/del(7q) status: -7/del(7q), n = 139; no -7/del(7q) n = 1338; no karyotype n = 153

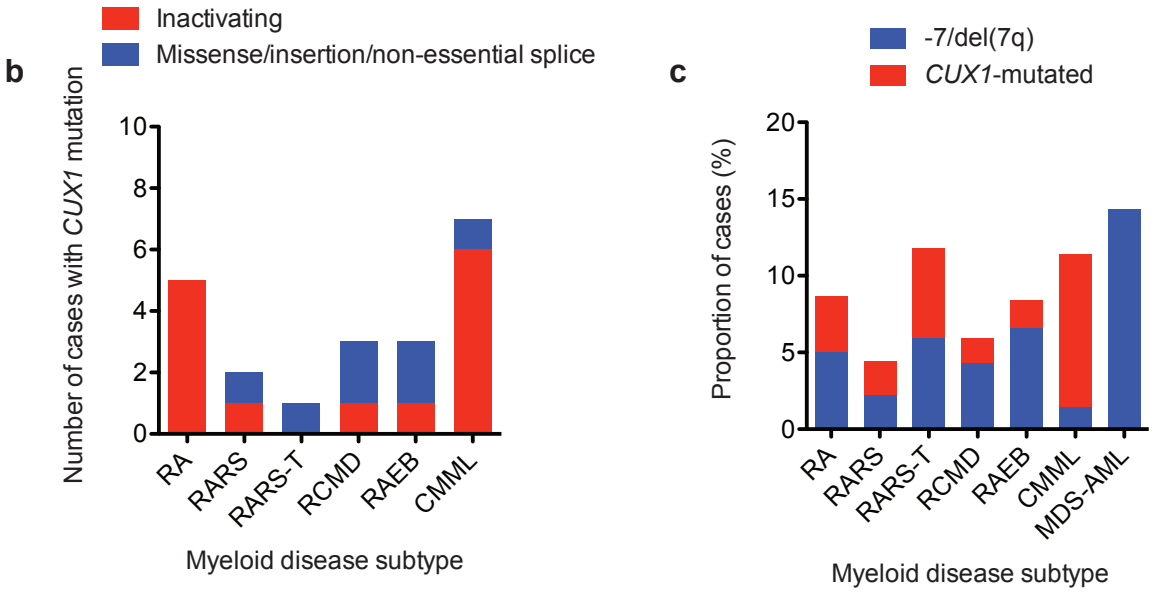

Supplementary Figure 1 | Characteristics of myeloid diseases cohorts.
(a) MPN subtype of 151 sequencing cases and characteristics of AML patient cohort (n = 1630).
(b) Distribution of *CUX1* mutations* across MDS and MDS/MPN subtypes is shown.
(c) Proportion of cases with *CUX1* or -7/del(7q) lesions according to disease subtype is shown.

RA, Refractory anemia; RARS, Refractory anemia with ring sideroblasts;
RARS-T, Refractory anemia with ring sideroblasts and thrombocytosis;
RCMD, Refractory cytopenia with multilineage dysplasia;
RAEB, Refractory anemia with excess blasts;
CMML, Chronic myelomonocytic leukemia;
MDS-AML, Acute myeloid leukemia with myelodysplasia-related changes
* Papaemmanuil, E. et al. Clinical and biological implications of driver mutations in myelodysplastic syndromes. Blood (2013). doi:10.1182/blood-2013-08-518886

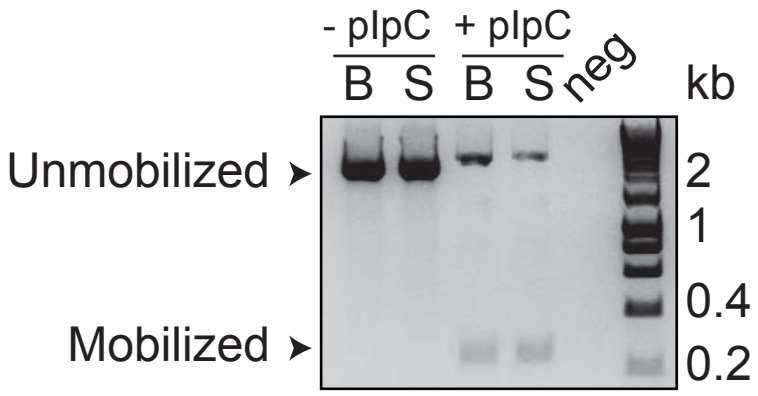

Supplementary Figure 2 | PCR verification of transposon mobilization following pIpC administration.

~2.2-kb and 225-bp products indicate presence of unmobilized and mobilized transposons respectively. B, bone marrow ; S, spleen; neg, no DNA.

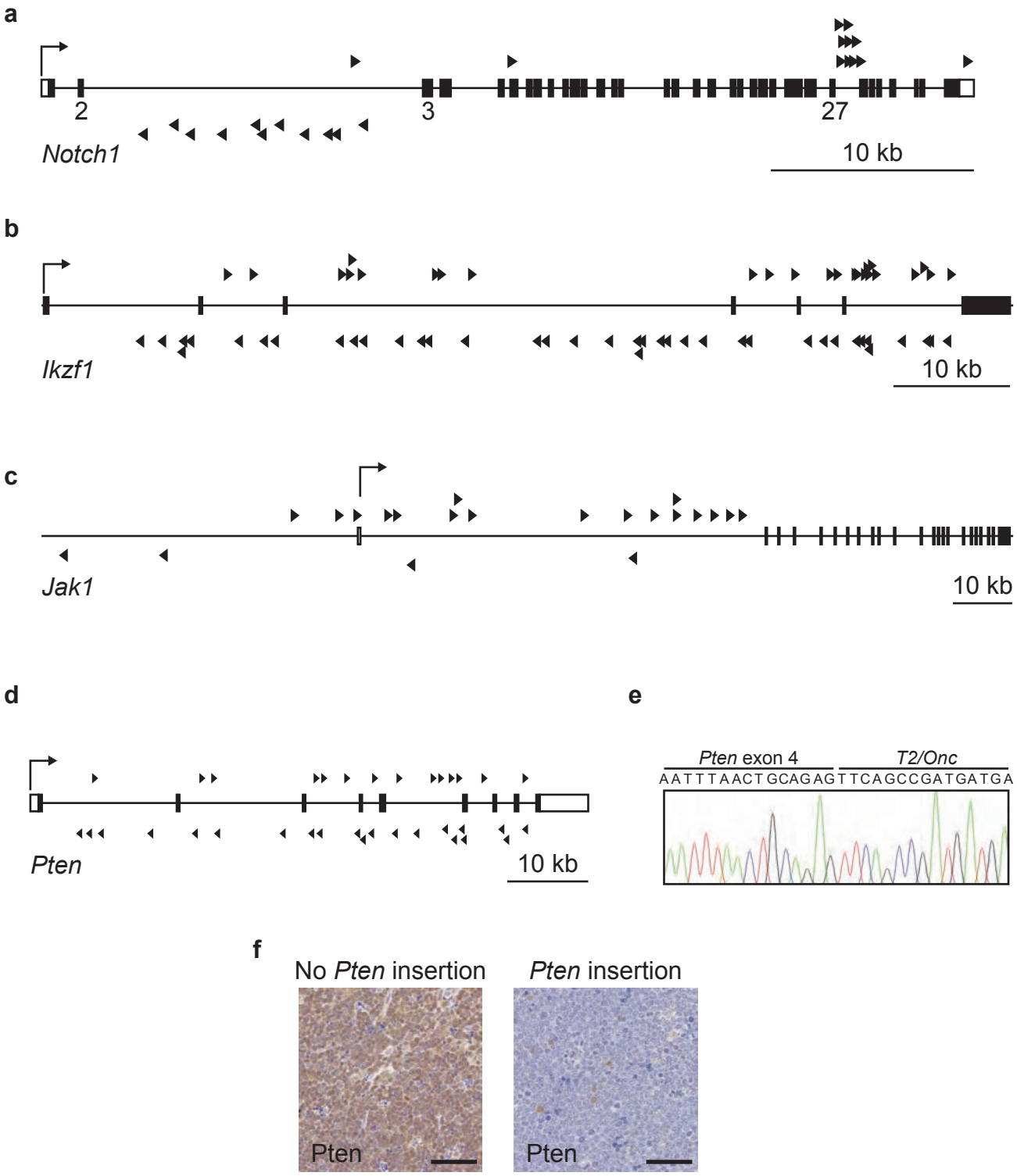

Supplementary Figure 3 | Pattern of insertion sites in mouse transposon tumors. **(a, b, c)** Transposon insertions within *Notch1* (**a**), *Ikzf1* (**b**) and *Jak1* (**c**) are shown by arrowheads. Direction of gene transcription is left-to-right. White boxes, non-coding exons; black boxes, coding exons. Direction of arrowheads indicate orientation of transposons. Insertions in *Notch1* and *Jak1* are predicted to be activating compared to inactivating insertions in *Ikzf1*. **(d)** Sense and antisense insertions in *Pten*. **(e)** Detection of splicing from *Pten* exon 4 to*T2/Onc* transposon, leading to *Pten* truncation. **(f)** Absence of Pten staining by immunohistochemistry in a transposon thymic tumor with *Pten* insertion. Scale bar = 50 μm.

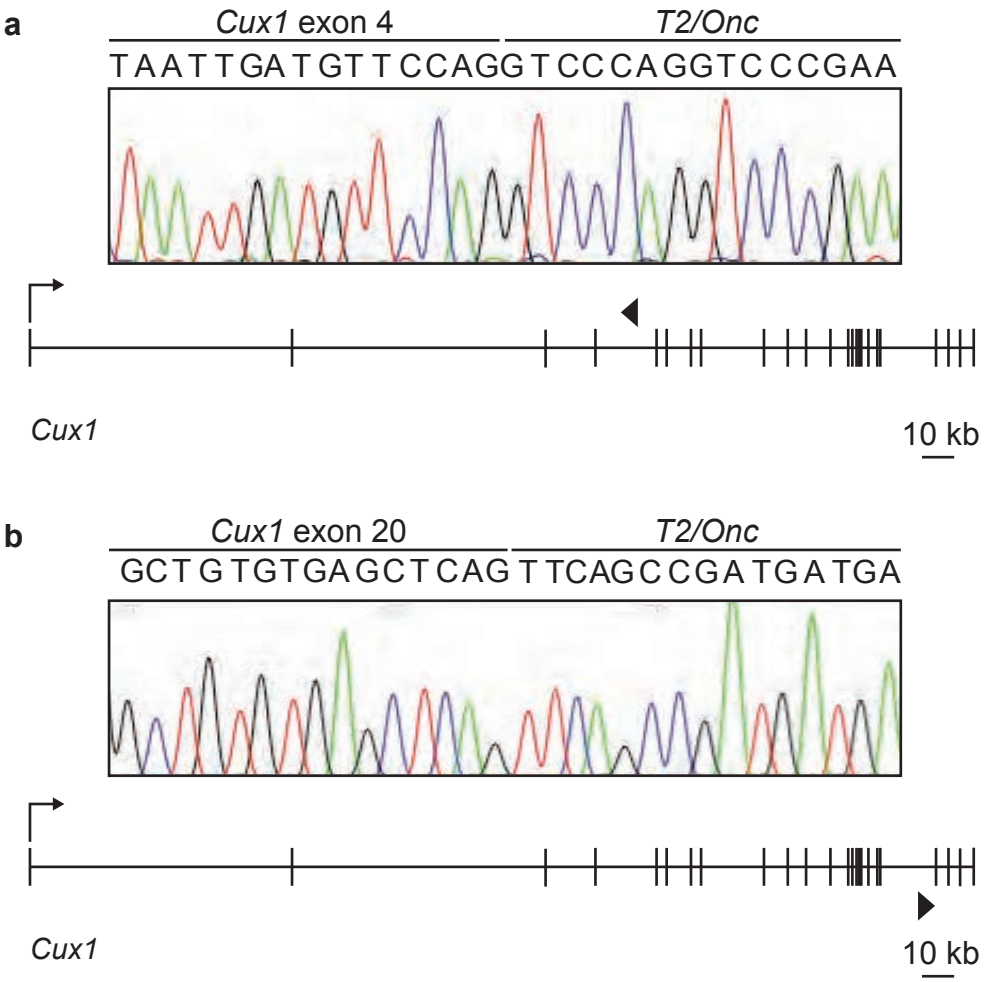

Supplementary Figure 4 | Verification of *Cux1-T2/Onc* splicing in transposon tumors. *S*plicing events involving *Cux1* exons 4 (**a**) and 20 (**b**) to the *T2/Onc* transposon were detected by sequencing of products obtained by RT-PCR using RNA from two transposon tumors. The location and direction of transposon insertions within *Cux1* are depicted below each sequencing trace.

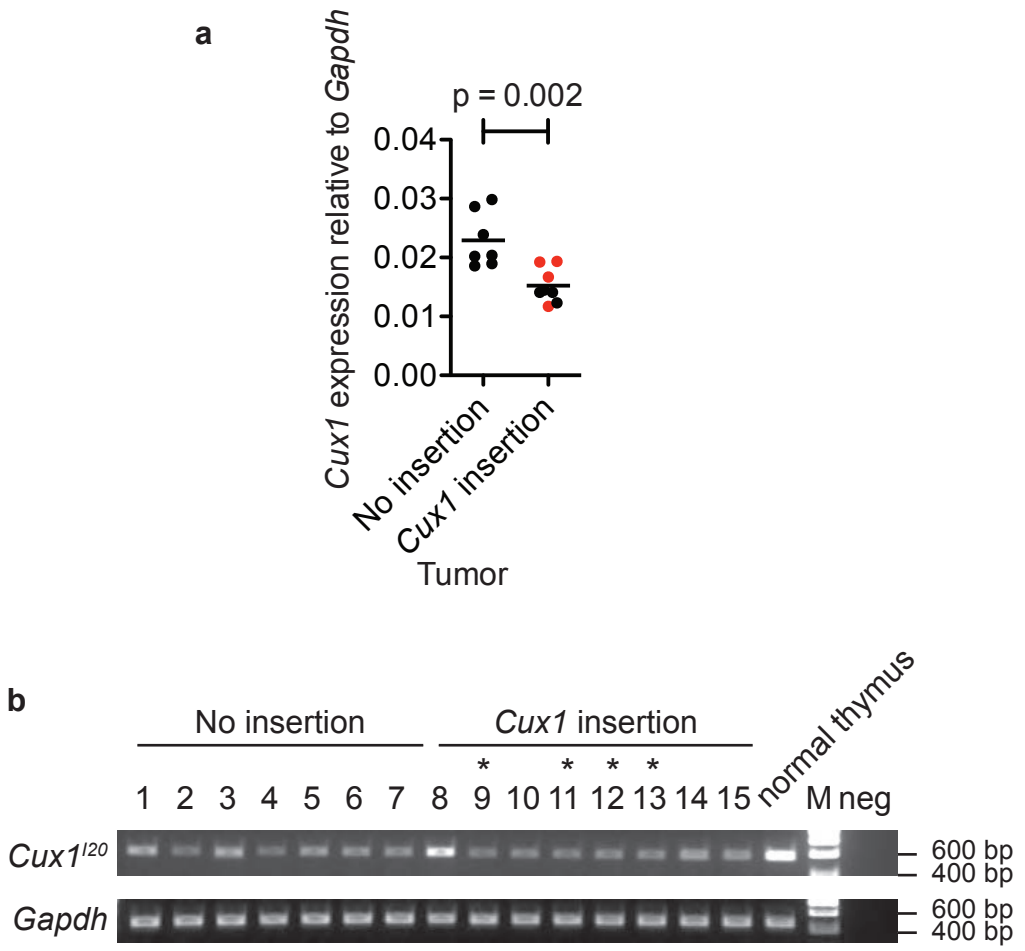

Supplementary Figure 5 | Expression of *Cux1* transcripts in mouse transposon tumors. **(a)** Reduction in *Cux1* expression in mouse transposon thymic tumors by qRT-PCR using Cux22F and Cux23R primers. Location of primers is shown in Fig. 2d. Primers detect all (*p75*, *p110* and *p200*) *Cux1* isoforms. Data show mean of triplicate measurements. Bar, group mean; p = 0.002, t-test. Red points show tumors with two *Cux1* insertions. **(b)** Semi-quantitative RT-PCR was performed on RNA isolated from mouse transposon tumors with and without *Cux1* insertions and normal thymus to detect $Cux1^{l20}$ encoding $Cux1^{p75}$. *Gapdh* expression was assessed as a control. M, DNA marker; neg, no template control. * indicates tumors with *Cux1* insertions in a forward orientation.

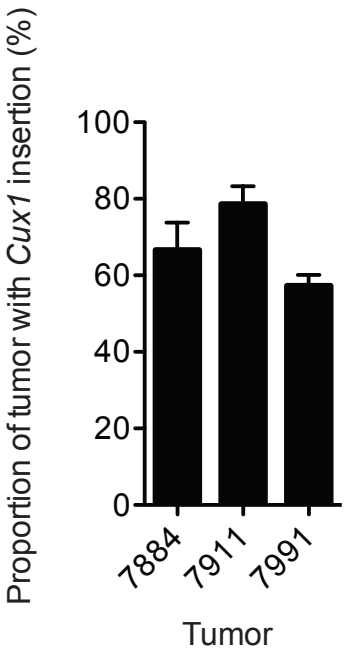

Supplementary Figure 6 | Quantification of *Cux1* insertions within tumors.
Quantitative PCR was performed on genomic DNA from three tumors to assess frequency of specific *Cux1* insertion events within each sample. Data show mean and s.e.m. from triplicate assessments.

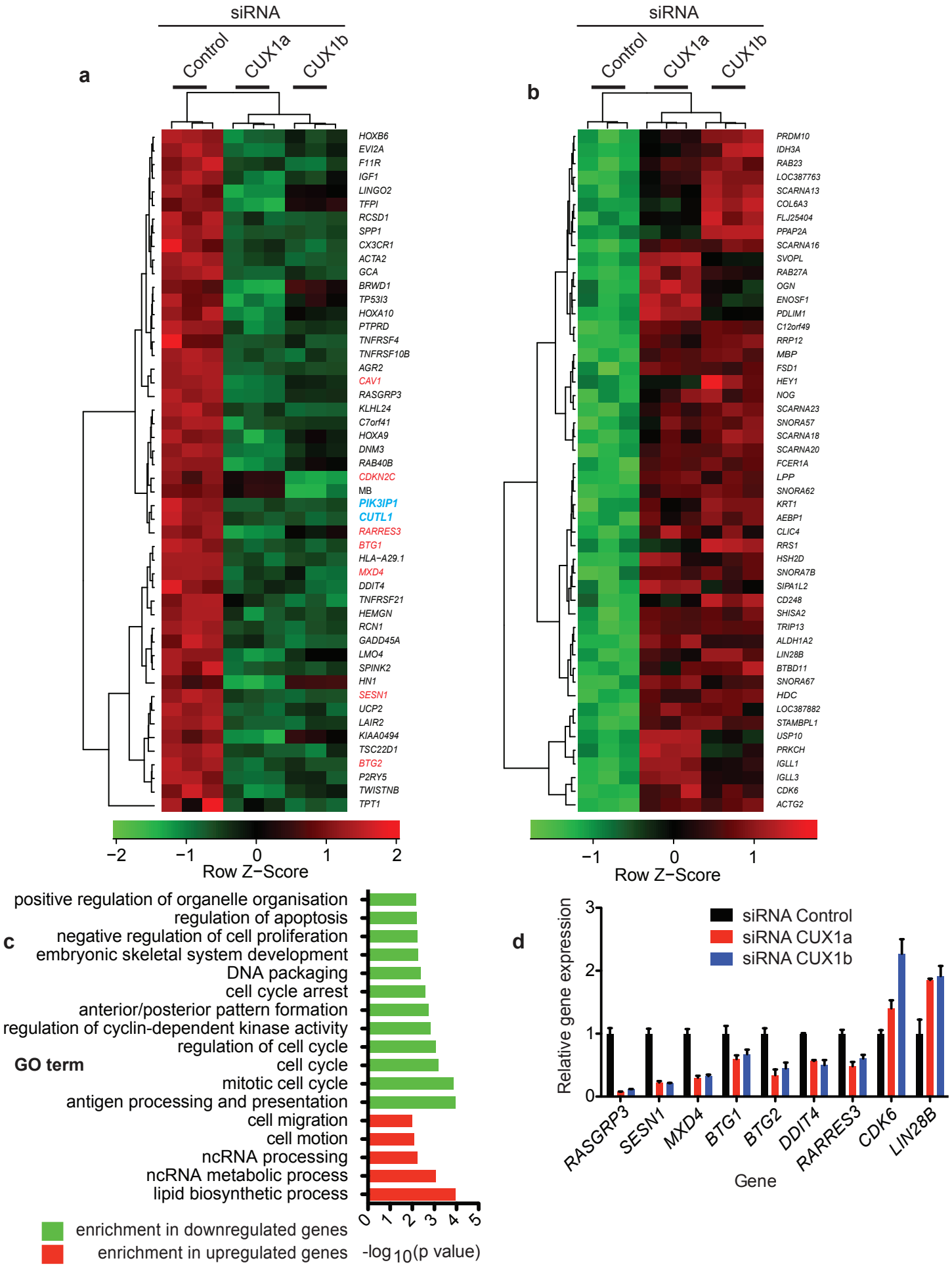

Supplementary Figure 7 | Enrichment in proliferation pathway signaling genes following CUX1 knockdown by siRNA in LOUCY cells.

(a, b) Heat maps showing uncensored hierarchical clustering of top 50 downregulated (**a**) and upregulated (**b**) genes following CUX1 knockdown using CUX1a and CUX1b siRNAs compared to control (n =3). Subset of proliferation pathway genes highlighted in red. *CUX1* (*CUTL1*) and *PIK3IP1* highlighted in blue. **(c)** Gene ontology (GO) analysis of dysregulated genes using DAVID. **(d)** Validation by qRT-PCR of CUX1-knockdown transcriptome profiling results. Data represent mean + s.d. (n =2).

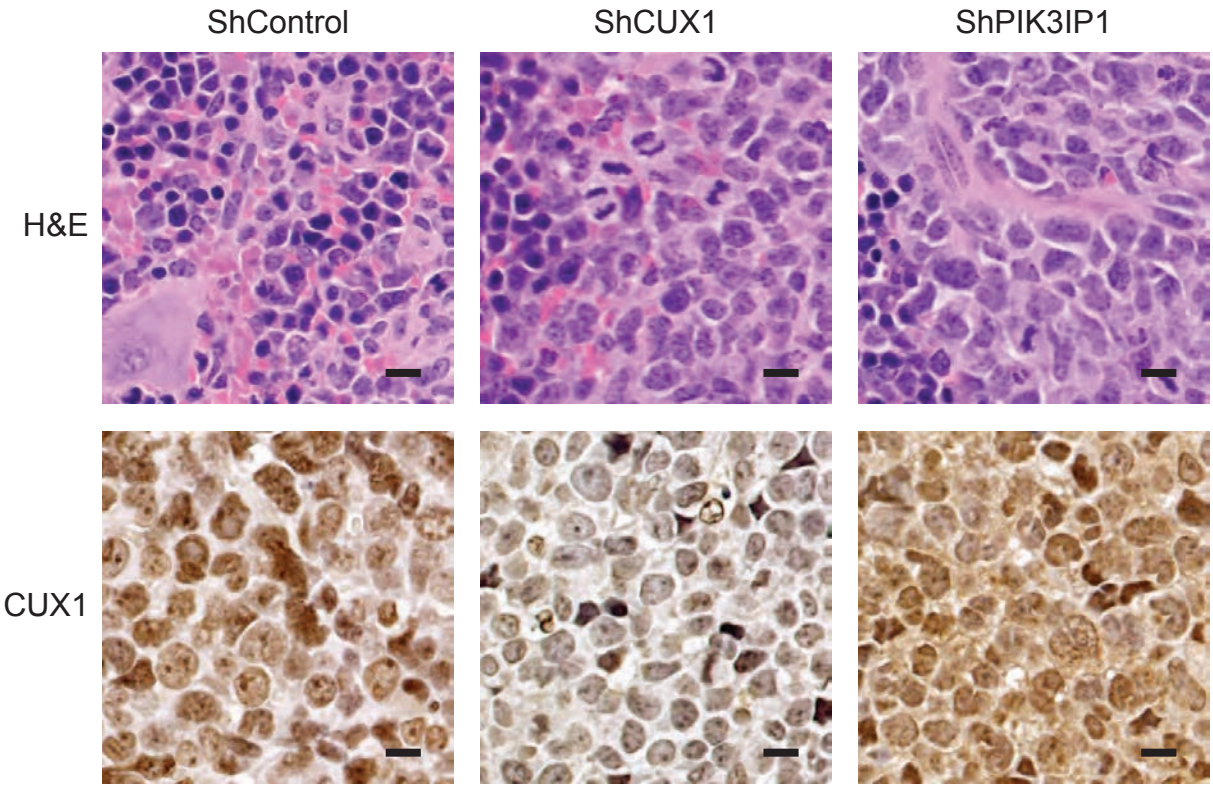

Supplementary Figure 8 | Histopathology of xenograft tumors.
Top: spleen sections from NOD-SCID mice injected with KE37 cells transduced with indicated knockdown vectors were stained with haematoxylin and eosin (H&E). Bottom: tumor xenografts were processed for immunohistochemical staining with anti-Cux1 antibodies. Scale bar 10 μm.

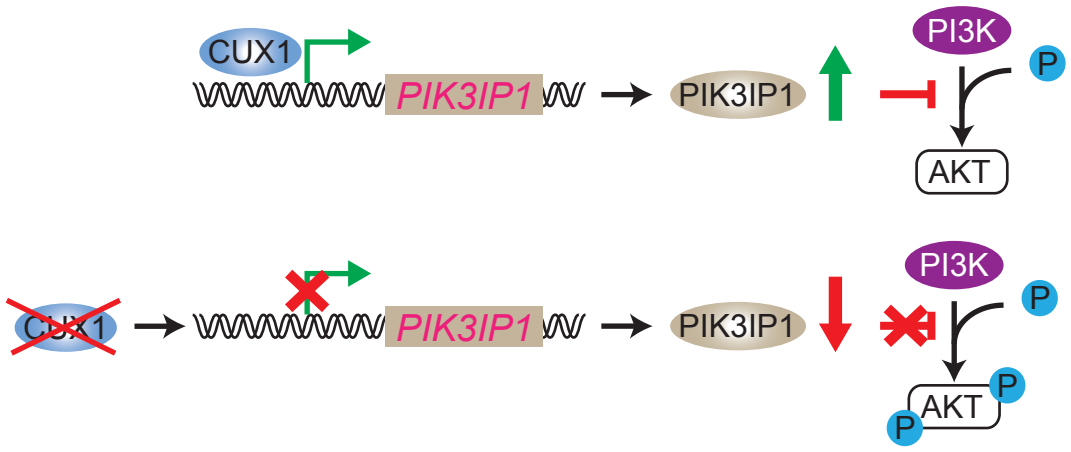

Supplementary Figure 9 | Model for role of CUX1 in driving PI3K signaling.

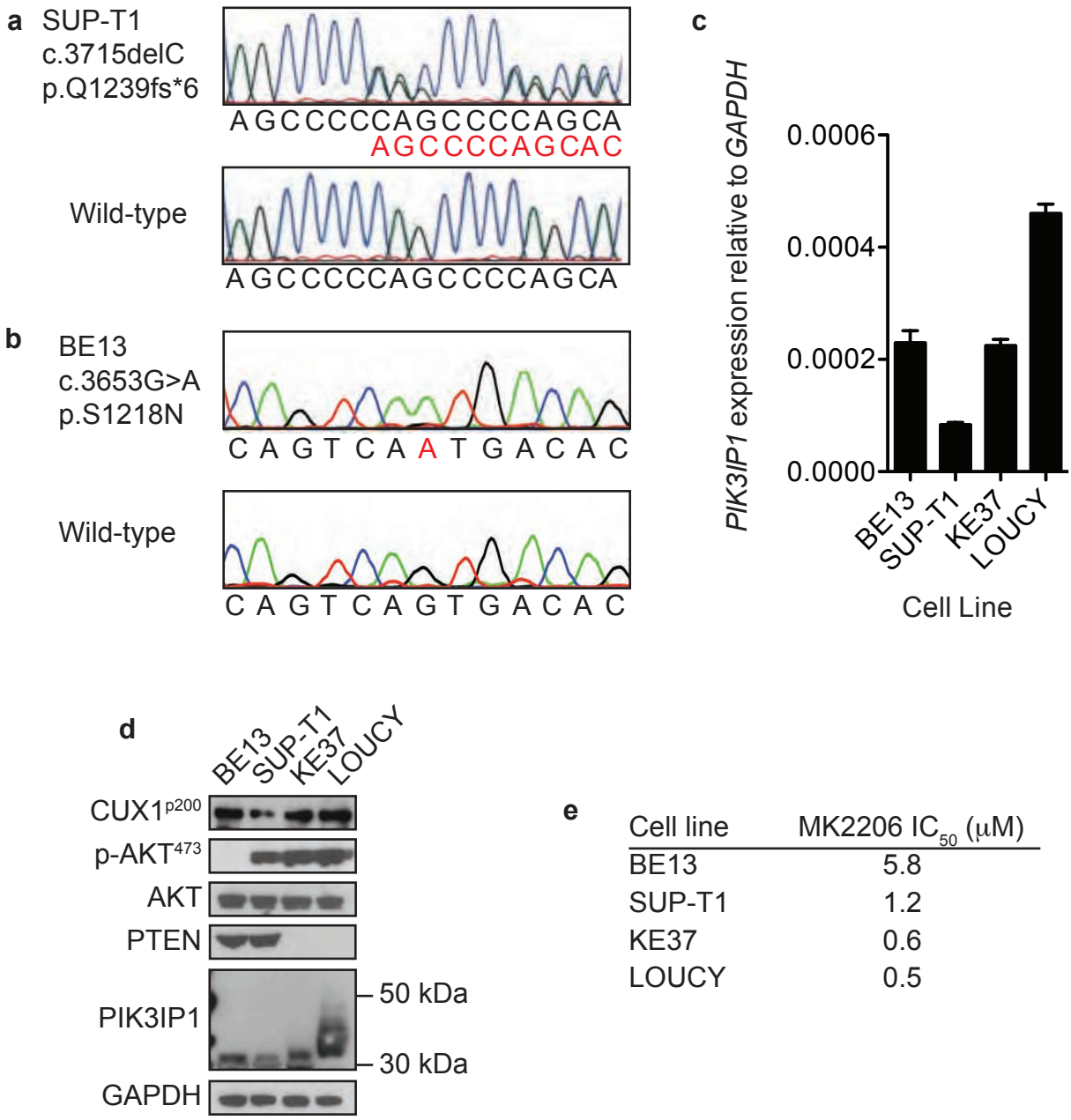

e

Cell line	MK2206 IC_{50} (μM)
BE13	5.8
SUP-T1	1.2
KE37	0.6
LOUCY	0.5

Supplementary Figure 10 | CUX1 and PIK3IP1 status in human T-ALL cell lines.
(a) The SUP-T1 line carries a heterozygous frameshift deletion mutation (c.3715delC) predicted to truncate CUX1. **(b)** The BE13 line harbors a homozygous missense change (c.3653G>A) predicted to generate p.S1218N change. **(c)** *PIK3IP1* expression was assessed by qRT-PCR in the indicated cell lines. Data are mean and s.e.m. of triplicate assessments. **(d)** Immunoblotting showing reduction in CUX1 and PIK3IP1 in SUP-T1 cells. PIK3IP1 shows marked retarded migration in LOUCY cells, attributable to protein glycosylation*. **(e)** Sensitivity of indicated cell lines to MK2206. IC_{50} values are shown. KE37 and LOUCY cells are PTEN-null and are sensitive to AKT inhibition. BE13 and SUP-T1 cells are *PTEN* wild-type. BE13 cells showed higher PIK3IP1 expression and undetectable phospho-AKT levels compared to SUP-T1 cells, suggesting that the homozygous missense *CUX1* mutation in these cells is inert and does not influence PIK3IP1 expression.

* Halim A, Nilsson J, Rüetschi U, Hesse C, Larson G. Human urinary glycoproteomics; attachment site specific analysis of N- and O-linked glycosylations by CID and ECD. Mol Cell Proteomics. 11: 10.1074/mcp.M111.013649, 1–17 (2012).

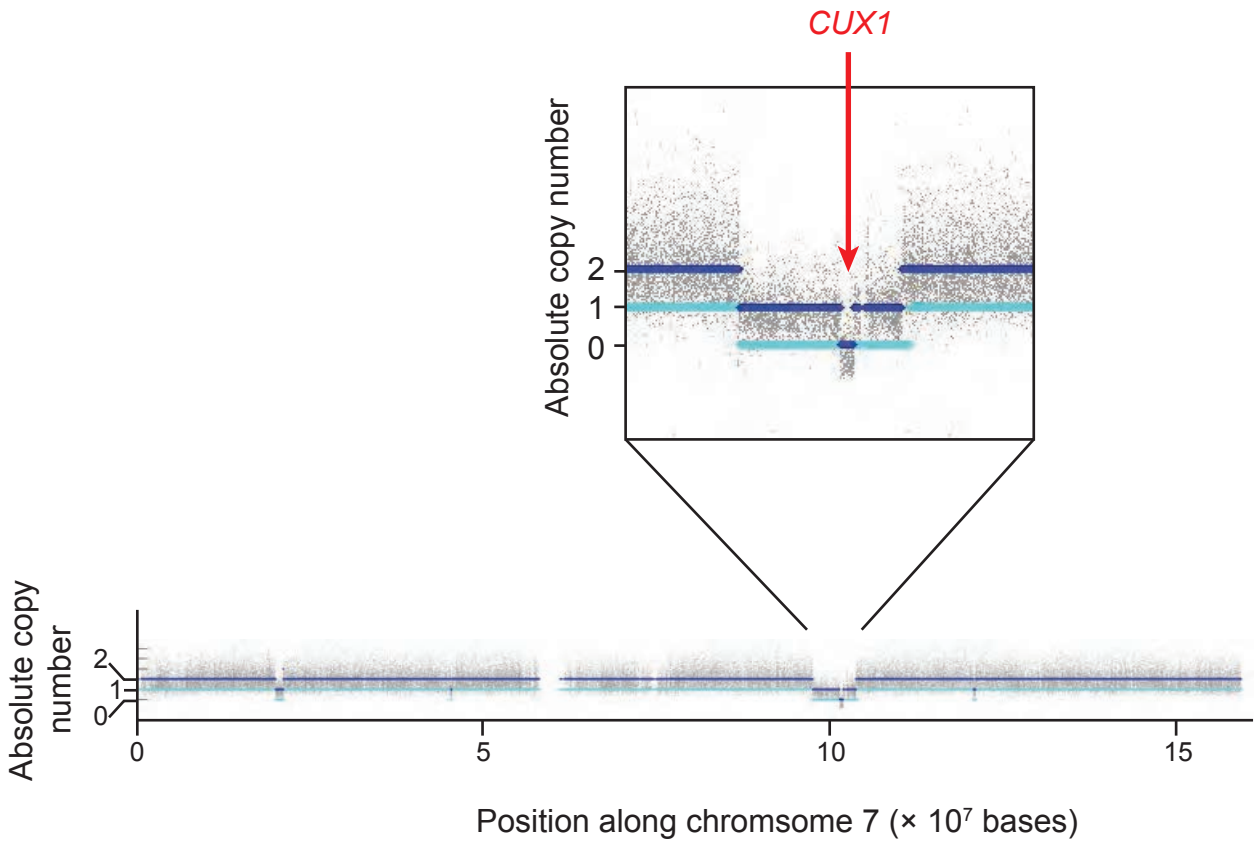

Supplementary Figure 11 | Focal homozygous *CUX1* deletion in H2803 mesothelioma cells. Absolute copy number plot of chromosome 7 using Affymetrix SNP 6.0 data demonstrating focal homozygous genomic deletion encompassing *CUX1* alone (dark blue line).

Cell line	NVP-BEZ235 IC_{50} (nM)
KE37::shControl	20.0
KE37::shCUX1	8.0

Cell line	MK2206 IC_{50} (μM)
MSTO-211H	0.3
H2803	1.0
MFE-280	1.4
H2810	8.6
H2804	11.6
NCI-H28	28.3
IST-MES1	36.8

Supplementary Figure 12 | Sensitivity of CUX1-deficient cell lines to NVP-BEZ235 and MK2206.
Dose response curves were derived from viability measurements of indicated cell lines after treatment with NVP-BEV235 or MK2206 drugs and used to calculate IC_{50} values.